Earthquake Engineering, Tenth World Conference © 1994 Balkema, Rotterdam. ISBN 90 5410 060 5

Dynamic impedances of bridge abutments

E. Alarcón & M. S. Gómez-Lera
Technical University of Madrid, José Gutiérrez Abascal, Spain

A. Martínez
Carlos Fernández Casado, Oficina Técnica, Madrid, Spain

Abstract.- The soil-structure interaction at bridge abutments may introduce important changes in the dynamic properties of short to medium span bridges. The paper presents the results obtained, through the use of the Boundary Element Method (B.E.M.) technique in several typical situations, including semiinfinite and layered media. Both stiffness and damping properties are included.

1. INTRODUCTION

The influence of approaching embankments on the behavior of bridges has been recognized since long ago. And this happens both at the ultimate limit state and while "in service" conditions. Even current codes (ref.1) recommend to simulate the superestructure-infraestructure interaction by modeling the abutments by suitable equivalente springs althrough no specific procedures or figures are suggested.

That the influence has to be important can be assessed qualitatively simply by looking at current designs. Fig. 1, for instance, is a recently designed short bridge of the integral abutment type.

It is easy to see that in order to have a good model it is unavoidable to include the infraestructure behavior both in the longitudinal and transverse directions. A quantitative estimate of the importance of the effect can be obtained using an equivalent single degree of freedom system following the ideas described by Wolf. To the typical model of reference 2 a spring and dashpot system has been added. The model is similar to that of reference 3 altough no gap has been included between the deck and the abutment i.e: we are refering to integral deck-abutment bridges. The values k_a and C_a represent the stiffness and damping properties of the abutment-embankment system, while the soil-structure interaction at the column foundation is represented by the couples (k_h; C_h) (k_ϕ; C_ϕ) related to horizontal and rotational displacements. Following assumptions similar to those of reference 2 it is possible to show that the frequency of the single degree of freedom system can be written as

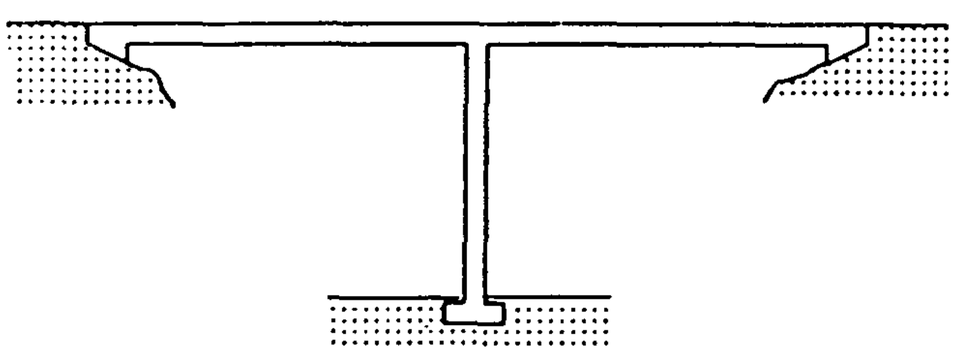

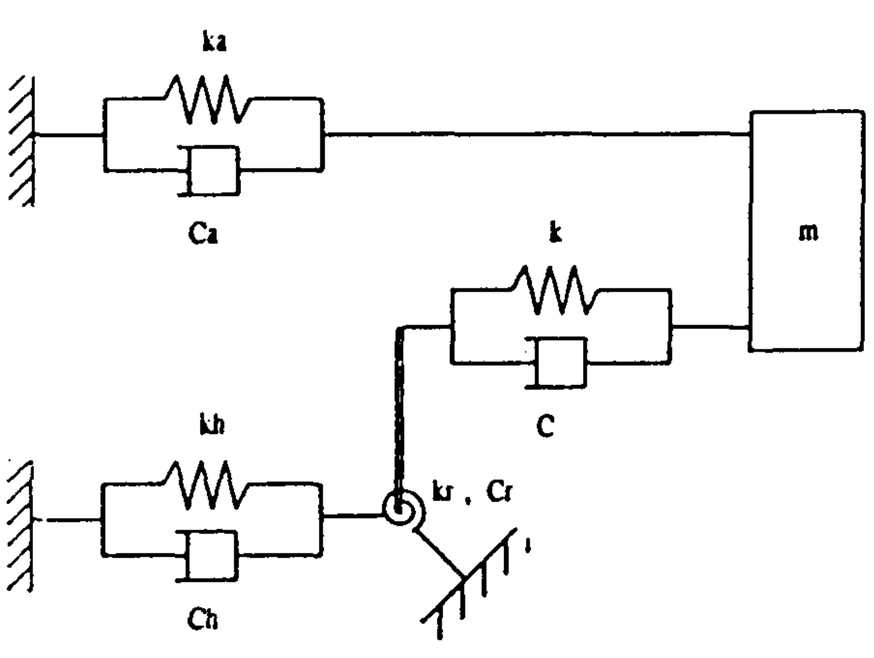

Figure 2

$$\omega^{*2} = \omega_a^2 + \frac{1}{\frac{1}{\omega_s^2} + \frac{1}{\omega_h^2} + \frac{1}{\omega_r^2}} \qquad (1)$$

Structure

$$\omega_a^2 = \frac{k_a}{m} \; ; \; \omega_s^2 = \frac{k}{m}$$

$$\omega_h^2 = \frac{k_h}{m} \; ; \; \omega_r^2 = \frac{k_r}{mh^2}$$

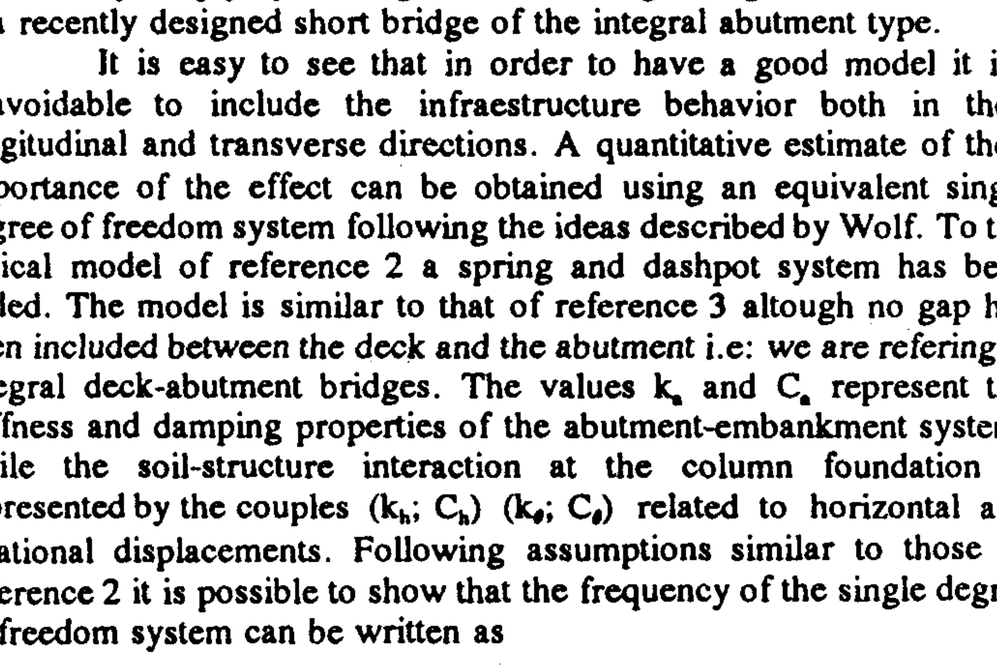

Figure 1

while the equivalent damping ratio is

$$\zeta^* = F_s\,\zeta + F_{so}\,\zeta_h + F_a\,\zeta_a \qquad (2a)$$

where F_s , F_{so} , F_a are factors corresponding respectively to the damping of the structure, soil damping and abutment damping. The definitions are

$$F_s = \frac{1}{1 + \omega_s^2 \left(\frac{1}{\omega_h^2} + \frac{1}{\omega_r^2} \right)}$$

$$F_{so} = \frac{1}{1 + \omega_h^2 \left(\frac{1}{\omega_s^2} + \frac{1}{\omega_r^2} \right)} \zeta_h + \frac{1}{1 + \omega_r^2 \left(\frac{1}{\omega_s^2} + \frac{1}{\omega_h^2} \right)}$$

$$F_a = \omega_a^2 \left(\frac{1}{\omega_s^2} + \frac{1}{\omega_h^2} + \frac{1}{\omega_r^2} \right) \qquad (2b)$$

and ζ, ζ_h , ζ_r , ζ_a are the damping ratios associated respectively to the structure, the horizontal soil displacement, the rotational soil displacement and the top of the abutment displacement.

In order to simplify the analysis the values proposed in reference 1 have been taken to obtain

$$\frac{k_r}{h^2\,k_h} = 0.8\,\left(\frac{L}{h}\right)^2 \;;\; \frac{\zeta_r}{\zeta_h} = 0.26 \qquad (3)$$

where L is a characteristic length of the column foundation and h is the abutment height.

So depending on the ratio h/L it is possible to plot families like those of figure 3. In the horizontal axis the ratio k/k_h between the stiffness of the structure and that of the horizontal soil spring has been used while the family curves depend on the ratio k_a/k between the abutment stiffness and that the structure.

In order to normalize the results, the ordinates reflect the ratio

$$\frac{\omega^{*2}}{\omega_a^2 + \omega_s^2} = \frac{\omega_a^2}{\omega_a^2 + \omega_s^2} + \frac{1}{(\omega_a^2 + \omega_s^2)\left(\frac{1}{\omega_s^2} + \frac{1}{\omega_h^2} + \frac{1}{\omega_r^2}\right)} \qquad (4)$$

so when ω_a is null(that is when there is no deck-abutment connection) the lower curve is obtained reflecting the well knowwn effect of the reduction in frequency due to foundation flexibility while when the abutment is completely rigid we obtain a unit value. As can be seen the variation is substantial and a discretization ignoring the abutment influence can be complete unconservative.

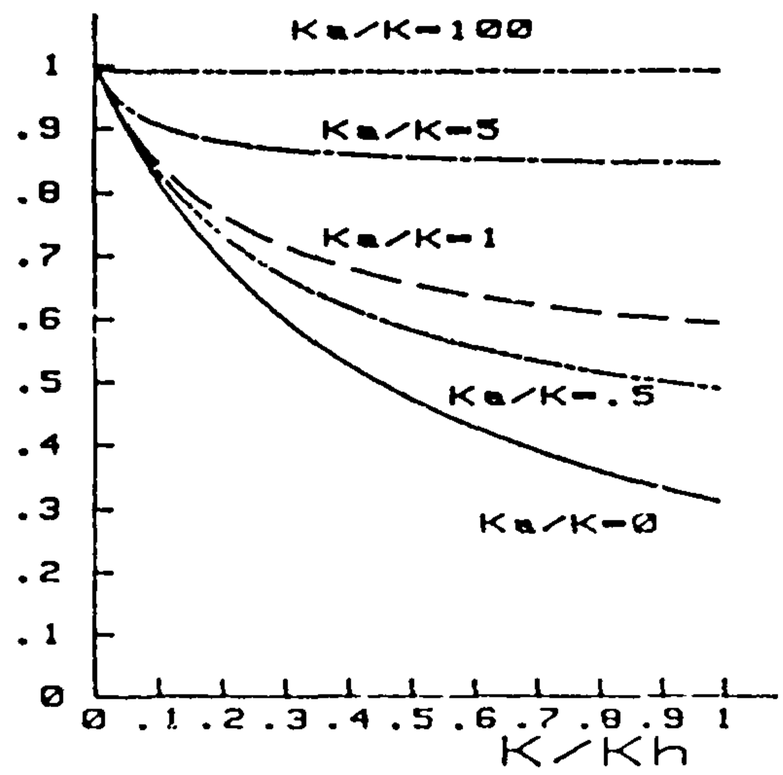

Figure 3

The weight of the abutment damping can be understood if we compare the factor afecting ζ_a in eq.2 with the factor afecting ζ and the one of ζ_h once the simplifications of eq.3 have been done. Those ratios are presented in figure 4 where it is clearly seen that the importance of ζ_a is substantial so that correctly evaluating its value is a fundamental requisite for a good modelling.

In a recent paper (ref.4) Wilson and Tan recognized the problem and proposed a plane strain trapezoidal model on rigid base to simulate the static transverse behavior of the abutment-embankment system. They did not provide any clue about how to quantify the amount of damping but, when they tried to identify the properties of a bridge (Melolan Road Overpass) that suffered a moderate earthquake without apparent damage they reported two interesting findings: to produce time histories compatible with the observed one it was neccesary first to assume a soil shear modulus of about 1/3 of the static one and then to include a damping ratio betwen 0.27 & 0.65. Although they justified those values on the basis of a nonlinear soil behavior the results that are included below show that a linear viscoelastic behavior can justify them if the dynamic response is analyzed including a substantial part of the soil around the embankment.

The objective of the paper is then the parametric analysis of the longitudinal and transverse dynamic impedances of rigid walls acting over layered media representing both the embankment and the soil on which it is erected.

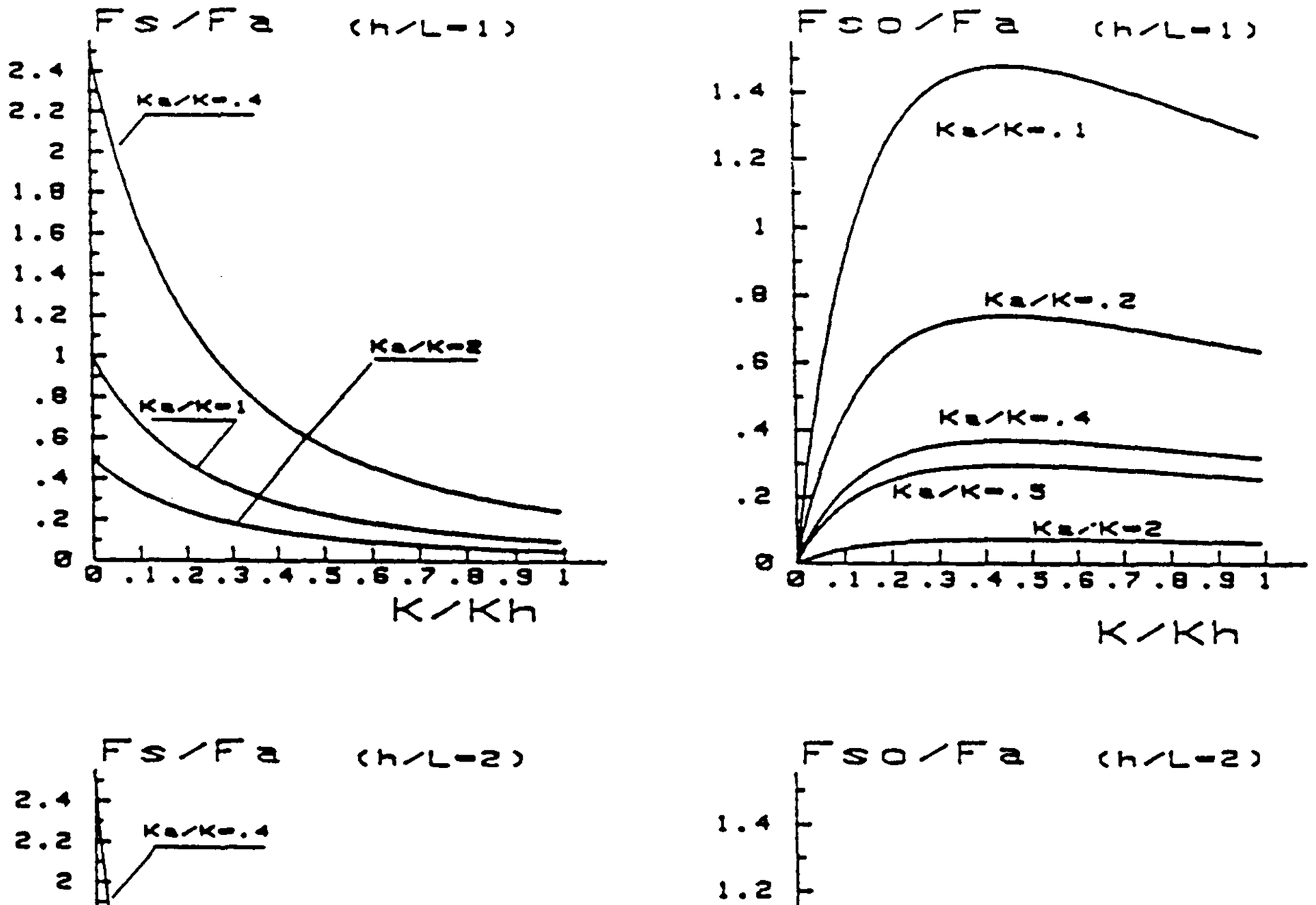

Figure 4a. Ratio of structure to abutment damping factors (F_s/F_a).

Figure 4b. Ratio of foundation to abutment damping factors (F_{so}/F_a).

2. NUMERICAL TECHNIQUE AND MODEL VALIDATION

As the main point is the computation of dynamic soil impedances the Boundary Element Method (B.E.M.) has been chosen as the numerical technique to be used in the parametric analysis. It has proved its efficiency in previous similar compromises, see for instance references 5 & 6, where some more details can be found.

The equations of motion are

$$(C_1^2 - C_2^2)\, u_{i,ij} + C_2^2\, u_{j,ij} + f_j = \frac{\partial^2 u_j}{\partial t^2}$$

$$C_1^2 = \frac{\lambda + 2G}{\rho}$$

$$C_2^2 = \frac{G}{\rho} \qquad (5)$$

where **u** is the displacement vector, **f** the body forces, ρ the material density and λ , **G** are the so-called Lamé parameters.

Moving to the frequency domain with **f** = **0** we obtain

$$(C_1^2 - C_2^2)\, u_{i,ij}^* + C_2^2\, u_{j,ij}^* + \omega^2\, u_j^* = 0 \qquad (6)$$

And it is possible to write an integral equation which on smooth boundaries looks as

$$\frac{1}{2} u_j^*(P) + \int_{\partial\Omega} T_{ji}^*(P,Q)\, u_i^*(Q) = \int_{\partial\Omega} T_{ji}^*(P,Q)\, t_i^*(Q) \qquad (7)$$

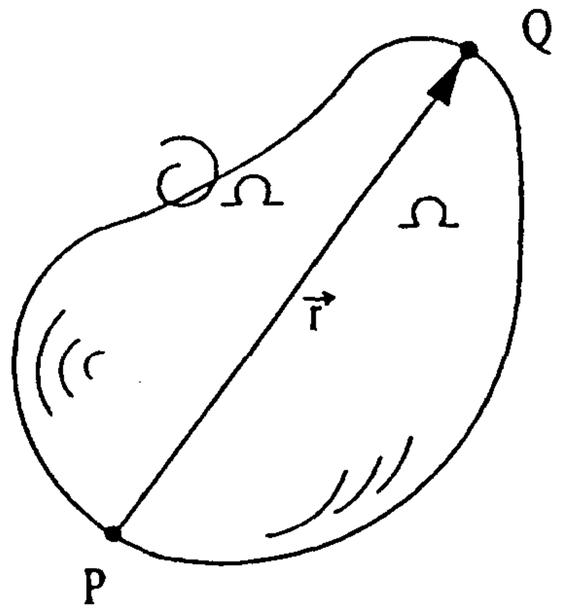

Figure 5

Where P and Q are points in the boundary (Fig.5). $\partial\Omega$ is the boundary of de domain Ω and T^*_{ji} ;

u^*_{ji} are influence tensors than can be writen as

$$u_{ij}^* = \frac{1}{\alpha\pi\rho C_2^2}(\psi\delta_{ij} - \chi r_{,i}\, r_{,j})$$

$$T_{ij}^* = \frac{1}{\alpha\pi}\left[\left(\frac{d\psi}{dr} - \frac{1}{r}\chi\right)\left(\delta_{ij}\frac{\partial r}{\partial n} + r_{,j}\, n_i\right) - 2\frac{d\chi}{dr} r_{,i}\, r_{,j}\frac{\partial r}{\partial n} - \frac{2}{r}\chi\,(n_j\, r_{,i} - 2\, r_{,i}\, r_{,j}\frac{\partial r}{\partial n}) + \left(\frac{C_1^2}{C_2^2} - 2\right)\left(\frac{d\psi}{dr} - \frac{d\chi}{dr} - \frac{2}{r}\chi\right) r_{,i}\, n_j\right] \tag{8}$$

where for bidimensional cases

$$\alpha = 2$$

$$\Psi = K_0\left(\frac{i\omega r}{C_2}\right) + \frac{C_2}{i\omega r}\left[K_1\left(\frac{i\omega r}{C_2}\right) - \frac{C_2}{C_1}K_1\left(\frac{i\omega r}{C_1}\right)\right]$$

$$\chi = K_2\left(\frac{i\omega r}{C_2}\right) - \left(\frac{C_2}{C_1}\right)^2 K_2\left(\frac{i\omega r}{C_1}\right) \tag{9}$$

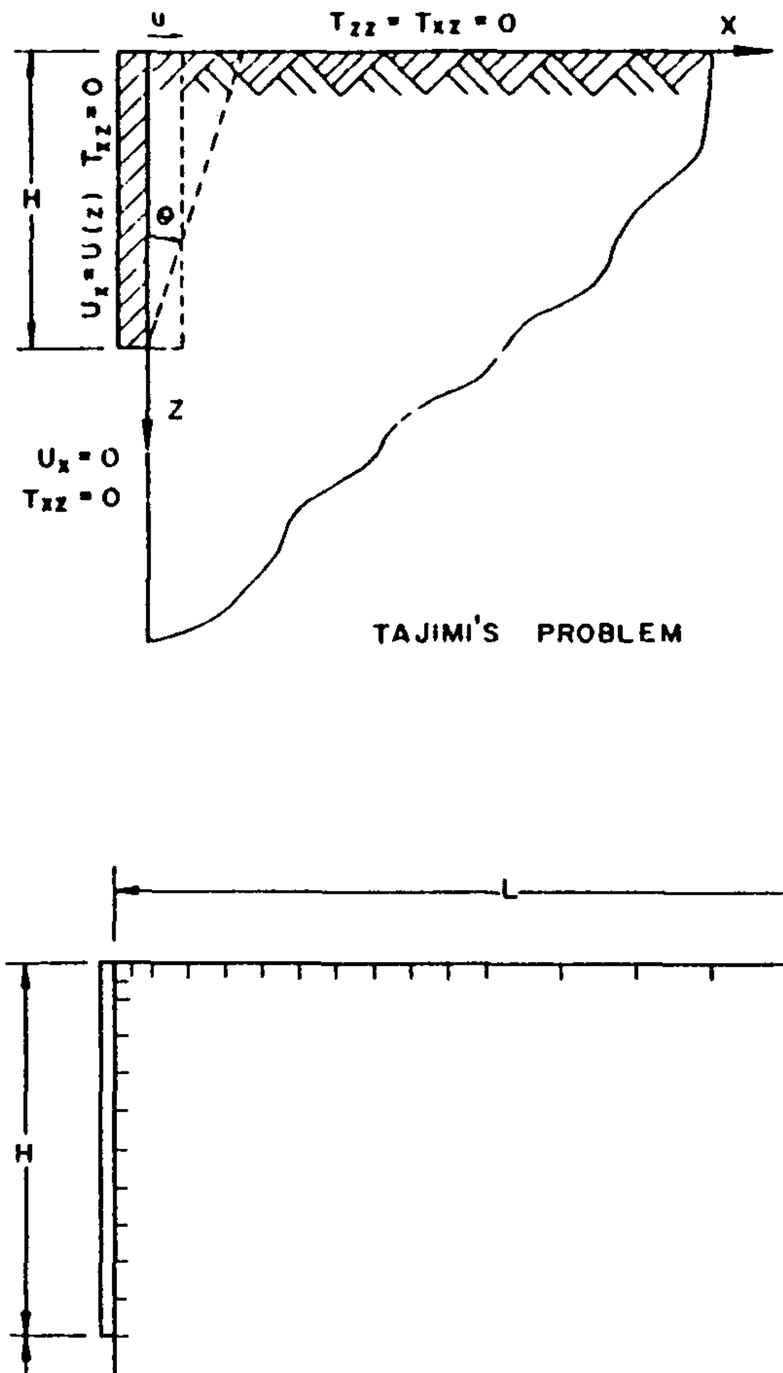

Figure 6a

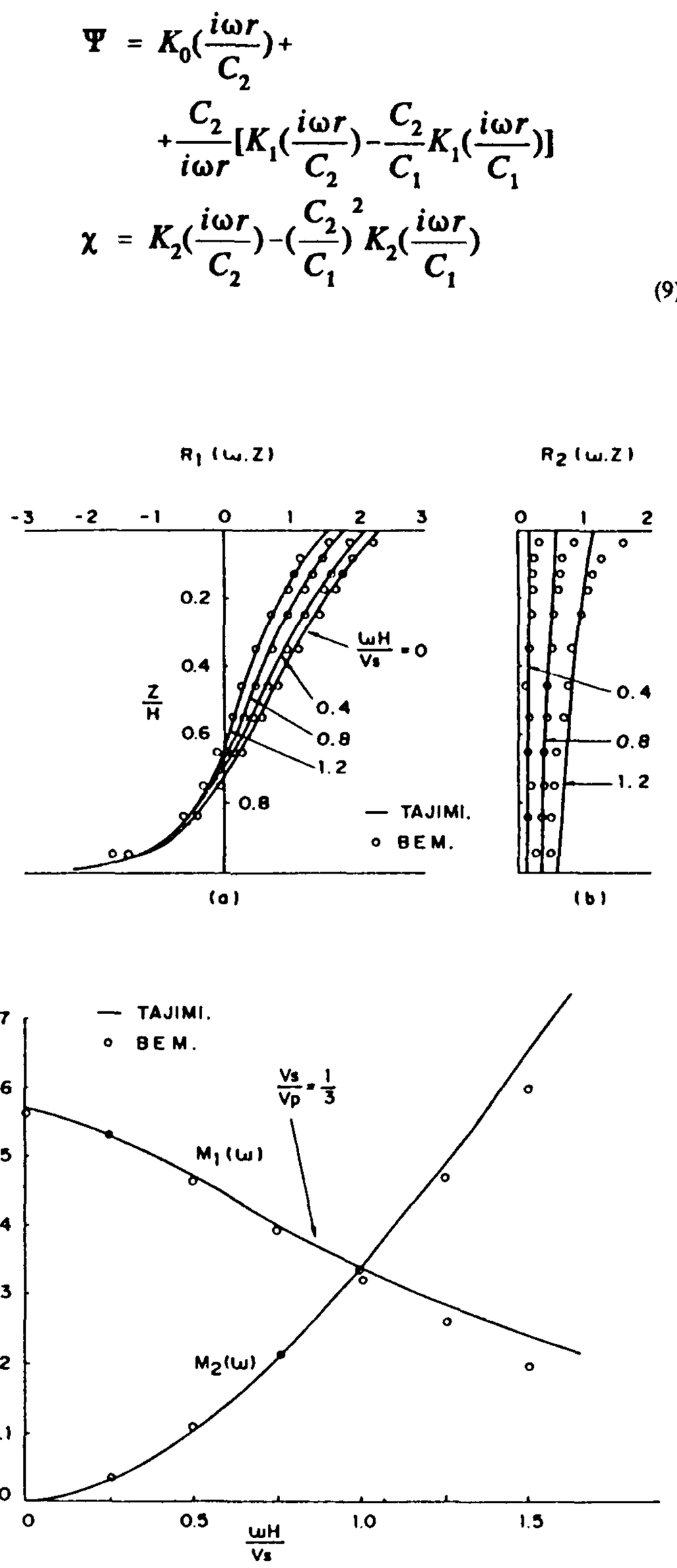

Figure 6b. Real and imaginary parts of the interface stresses(above) and acting moment(below).

and for three dimensional ones

$$\alpha = 4$$

$$\Psi = \frac{e^{\frac{-i\omega r}{C_2}}}{r} + \left(\frac{C_2}{i\omega r} - \frac{C_2^2}{\omega^2 r^2}\right)\frac{e^{\left(\frac{-i\omega r}{C_2}\right)}}{r} - \left(\frac{C_2}{C_1}\right)^2 \left(\frac{C_1}{i\omega r} - \frac{C_2^2}{\omega^2 r^2}\right)\frac{e^{\frac{-i\omega r}{C_1}}}{r}$$

$$\chi = \left(\frac{3C_2}{i\omega r} - \frac{3C_2^2}{\omega^2 r^2}\right)\frac{e^{\frac{-i\omega r}{C_2}}}{r} - \left(\frac{C_2}{C_1}\right)^2 \left(\frac{3C_1}{i\omega r} - \frac{3C_1^2}{\omega^2 r^2} + 1\right)\frac{e^{\frac{-i\omega r}{C_1}}}{r} \qquad (10)$$

where r is the distance between P and Q.

In order to check the accuracy and to test several modelling details (mesh size, element size, numerical integration type, etc) (ref.7) two classical works, relevant to the topic under discussion, have been used; in the first one (ref.8) Tajimi used a wave-propagation technique to analyze the response of quarter-space with a rigid corner inducing harmonic displacements and rotations. Figure 6 shows that a very simple mesh with "constans" boundary elements is able to reproduce accurately Tajimi's findings. The only precautions to be taken are related to the size element around the corner and at the bottom tip of the wall. Also the size of the discretized boundary and of the elements is related to the frequency of excitation so that an adaptive mesh (ref.6) can be used advantageously which length and size depends on the excitation wave length.

The same happens with figure 7 where the discretization corresponds to a problem proposed by Wood (ref.9). Here again both the real (stiffness) and imaginary (dissipation) parts of the impedance are reproduced without any problems.

With such a proverful technique it is an easy matter to analyze more complicated cases including the halfspace situation or the layered one. In figure 8 several meshes are included that are intended to be use both for a longitudinal as well as for a transverse situations. As can be seen the discretization includes the interfaces because a piece-wise heterogeneous soil is studied.

3. PARAMETRIC STUDY

Using the meshes shown in figure 8 several cases have been run varying the relative properties of the strata. For the longitudinal direction figure 9 show the behavior for a rocking imposed displacements. The parametric study includes the Poisson ratio variation and the rigid-bottom depth variation. As can be seen several oscilations related to the stratum natural frequency can be appreciated. The material damping was only 5 %. It is interesting to see that while the rotational stiffness is not very much affected by the bedrock depth, the damping value reflects the importance of the radiation in the last cases. For the transverse situation a Poisson coefficient of 0.3 has been selected and a 5 % material damping has been included in all models. The shear modulus of the stratum has been varied between 1 and 100 times that of the embankment and the proportion between the stratum depth P and the embankment height H has been varied between 0 and 3 times. Also a halfspace has been analyzed for completnes. In any case the crest embankment width has been taken as twice its height.

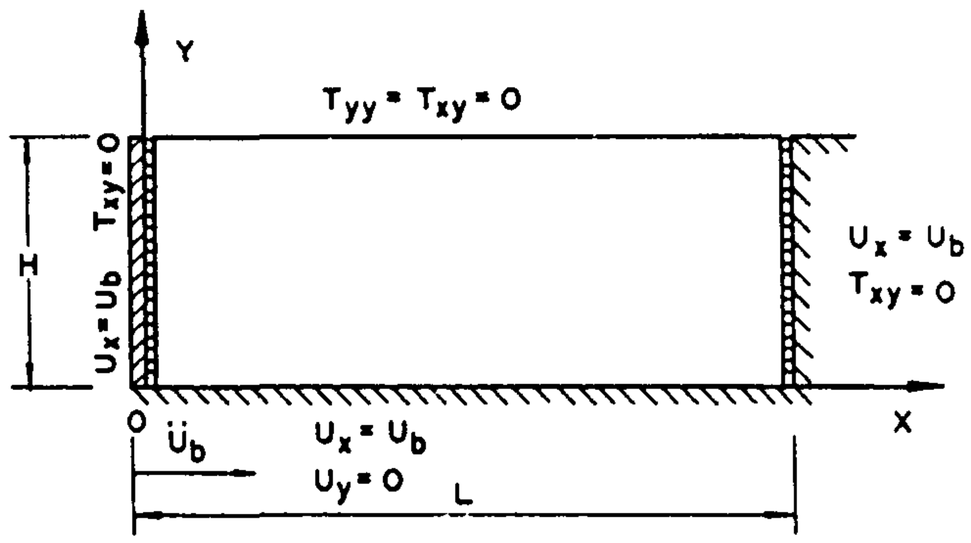

WOOD'S PROBLEM

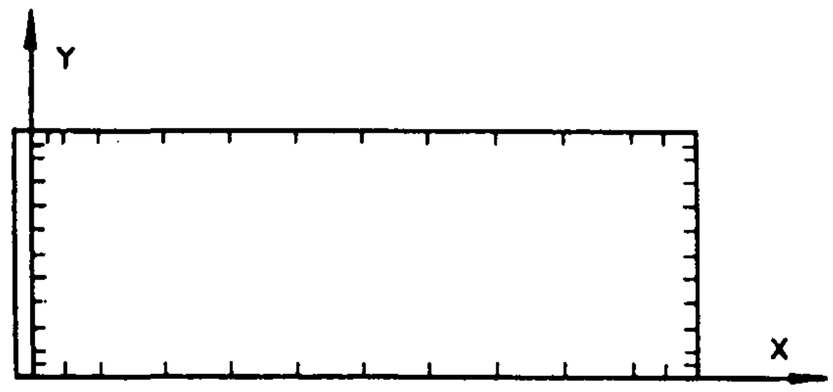

BEM MODEL.

L/H = 5.0

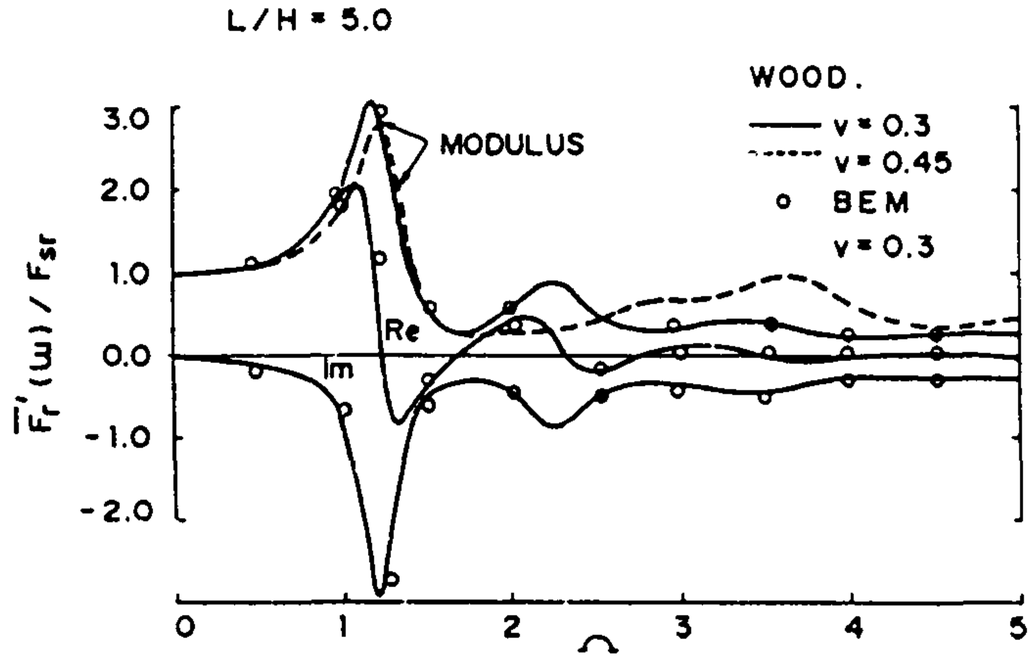

L/H = 5.0

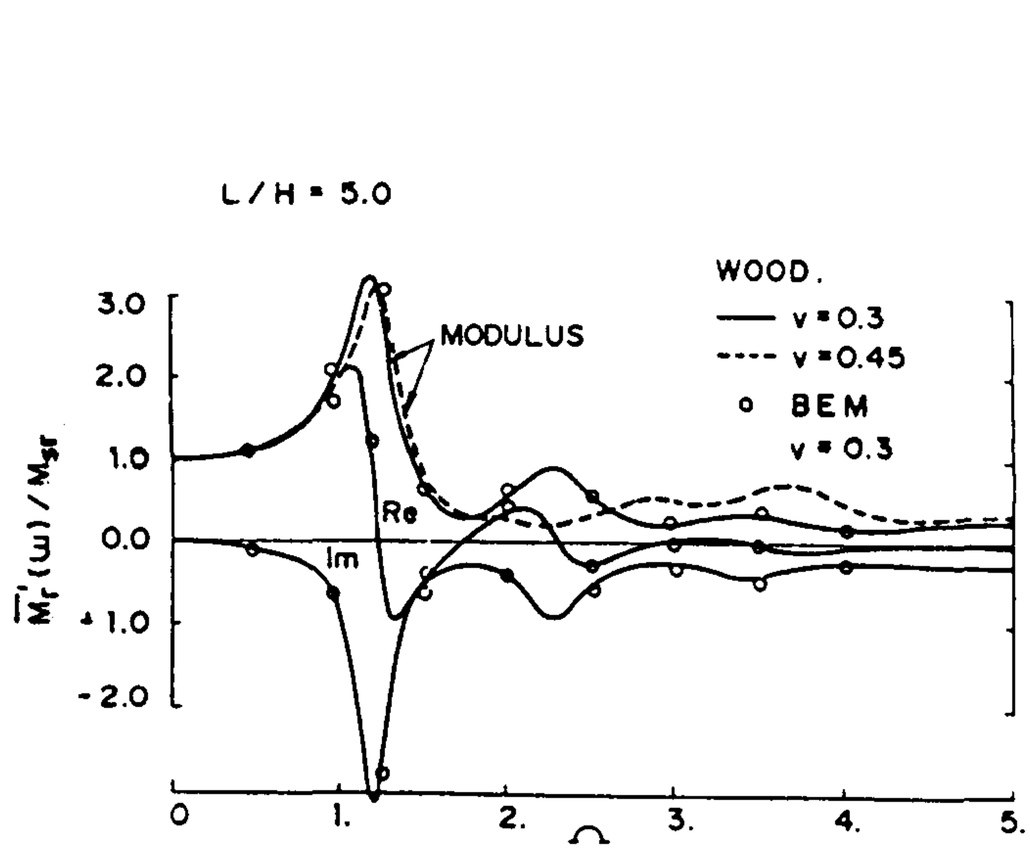

Figure 7

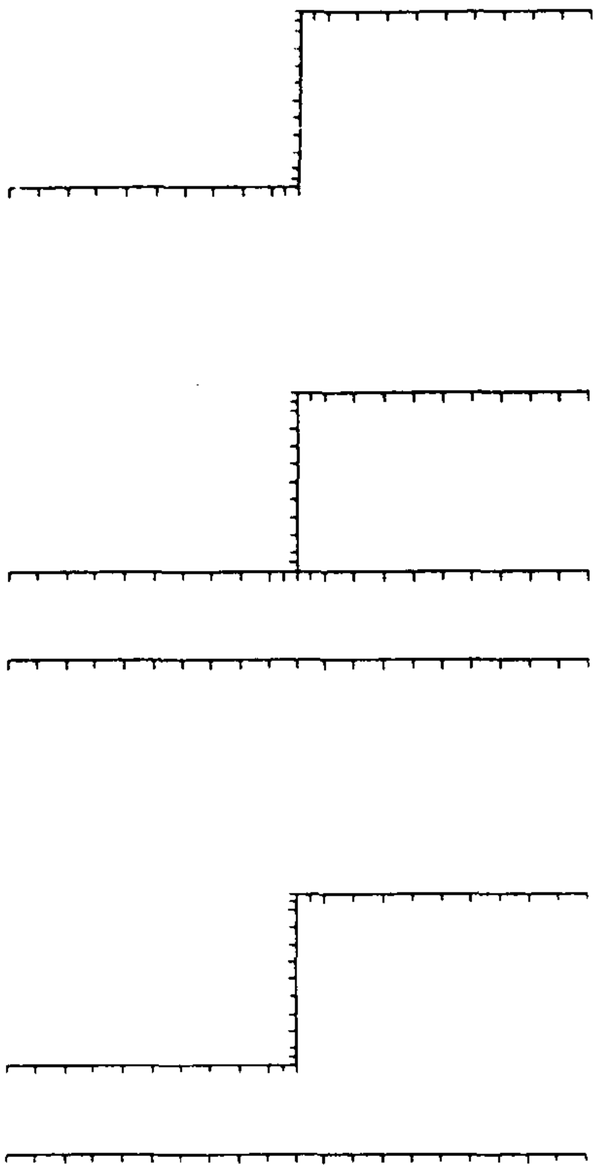

Figure 8a. Meshes used for longitudinal vibration

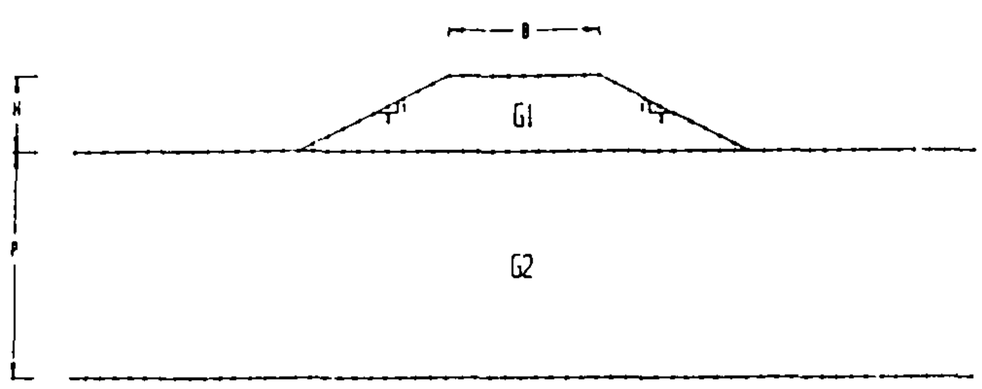

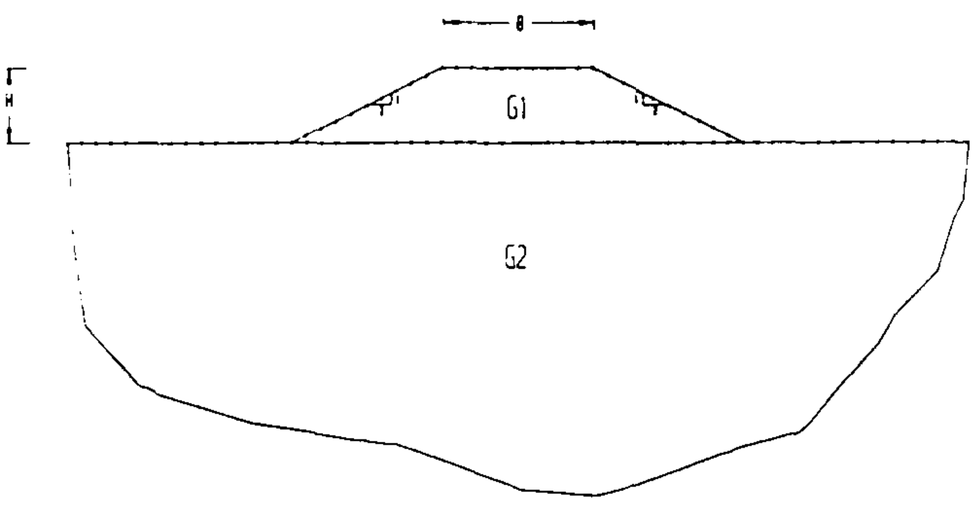

Figure 8b. Meshes used for transverse vibration

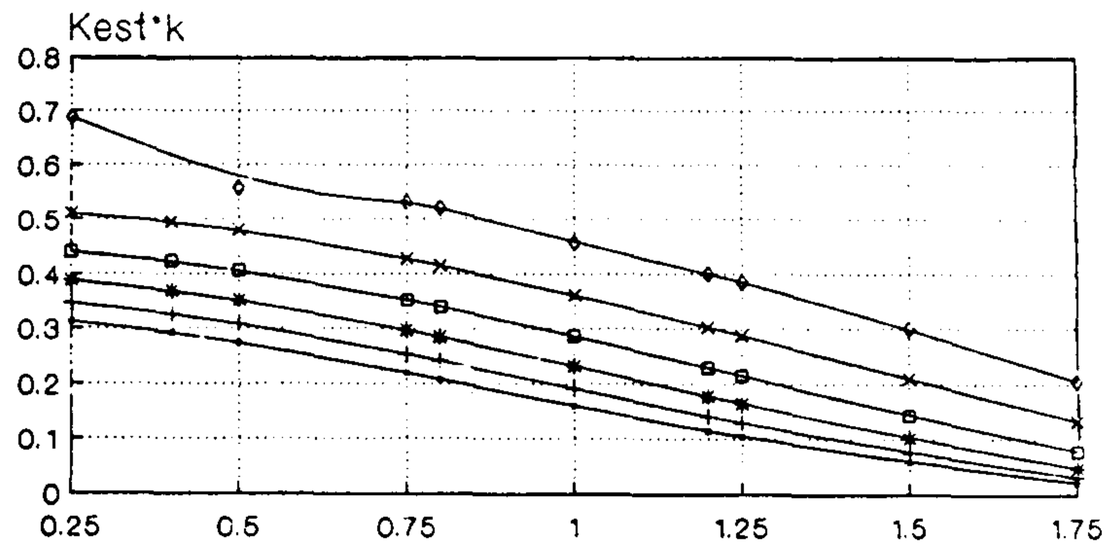

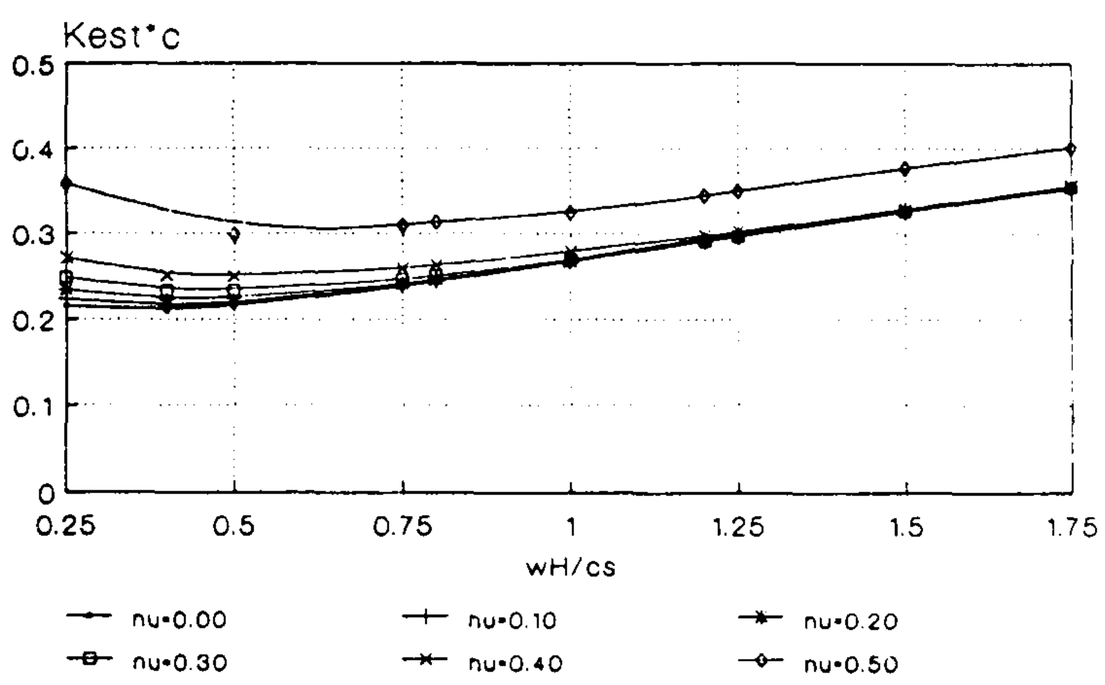

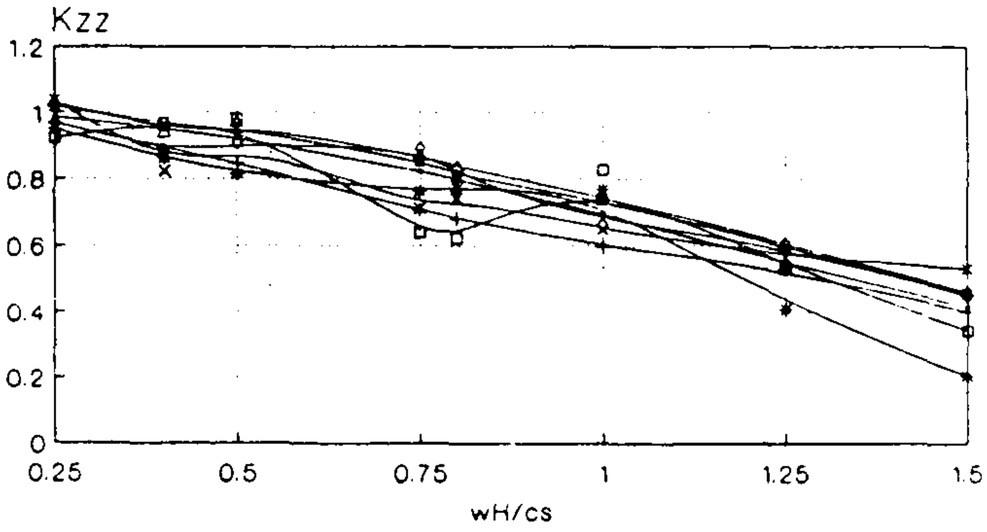

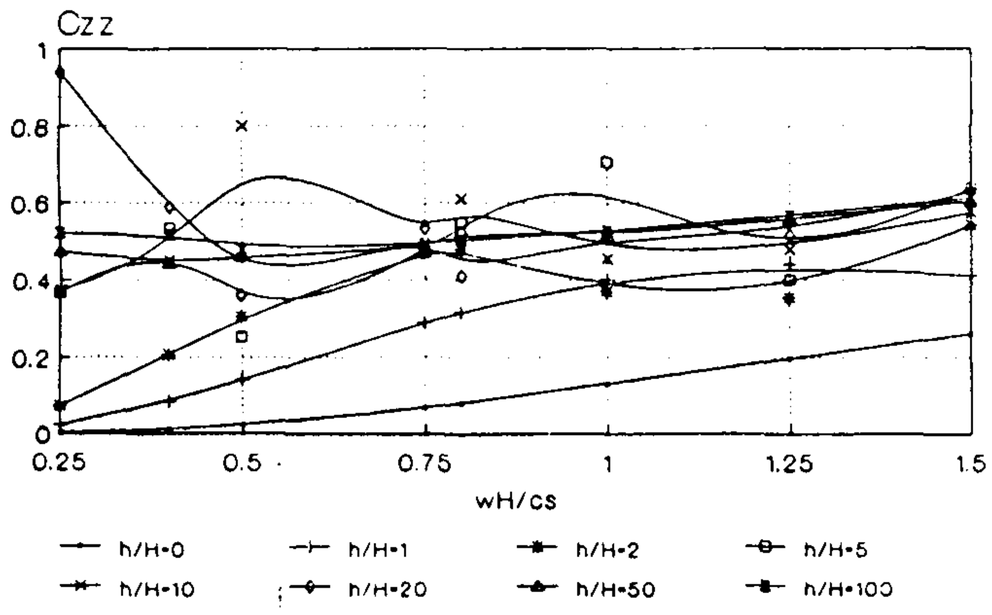

Figure 9

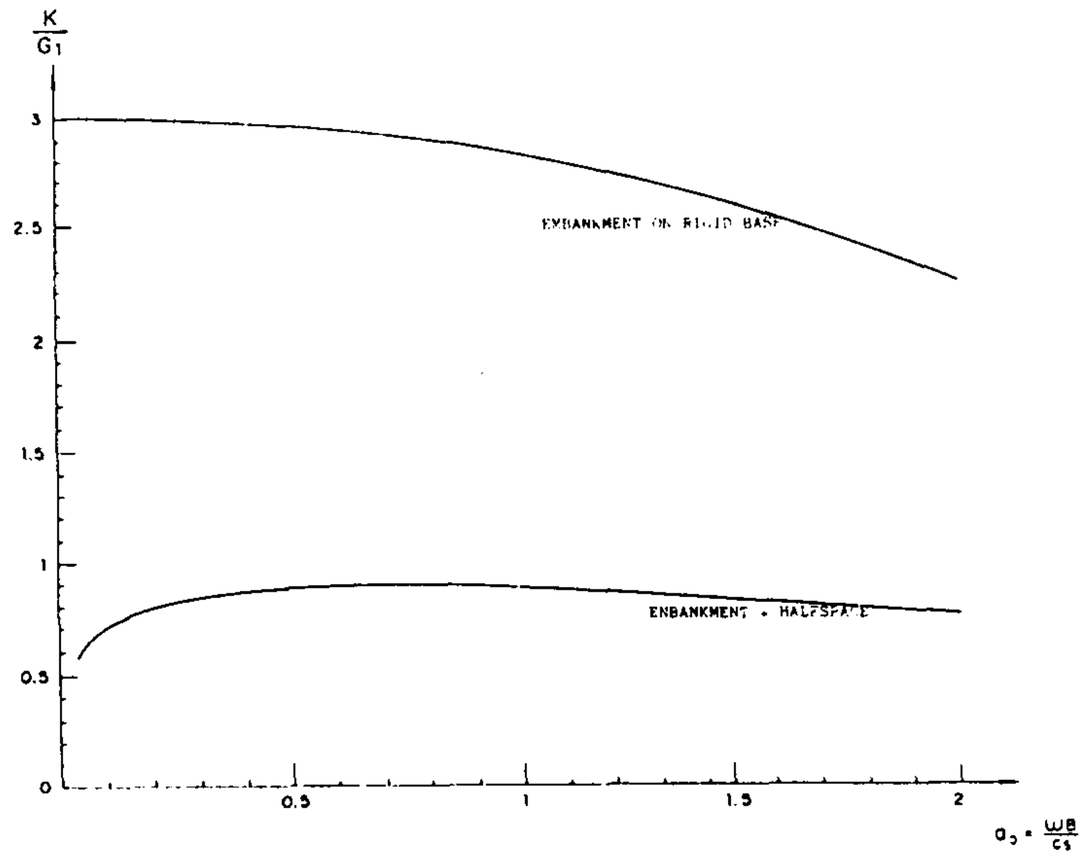

Figure 10. Horizontal stiffness

The real part (stiffness) of the impedances is plotted in figures 10, 11 and 12 for the cases of vertical, horizontal and rocking displacements. As can be seen when P diminishes or the modulus of the stratum increases the curves move towards the rigid base trapezoid case. It is interesting to notice the oscillations the horizontal stiffnees, around the halspace one. Also noticeable is the reduction of stiffness that is produced when the frequncy increases or when a halfspace or stratum is added under the trapezoid.

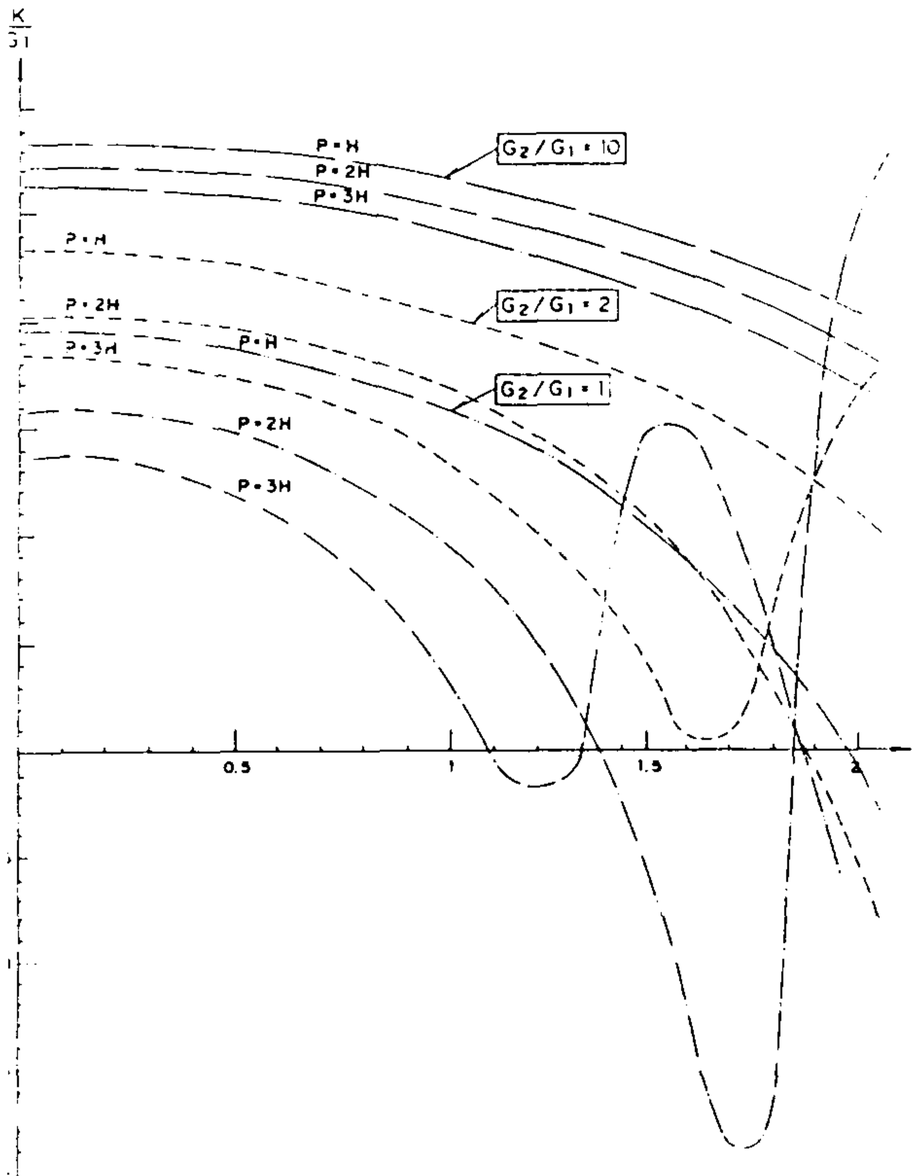

Figure 11. Horizontal stiffness

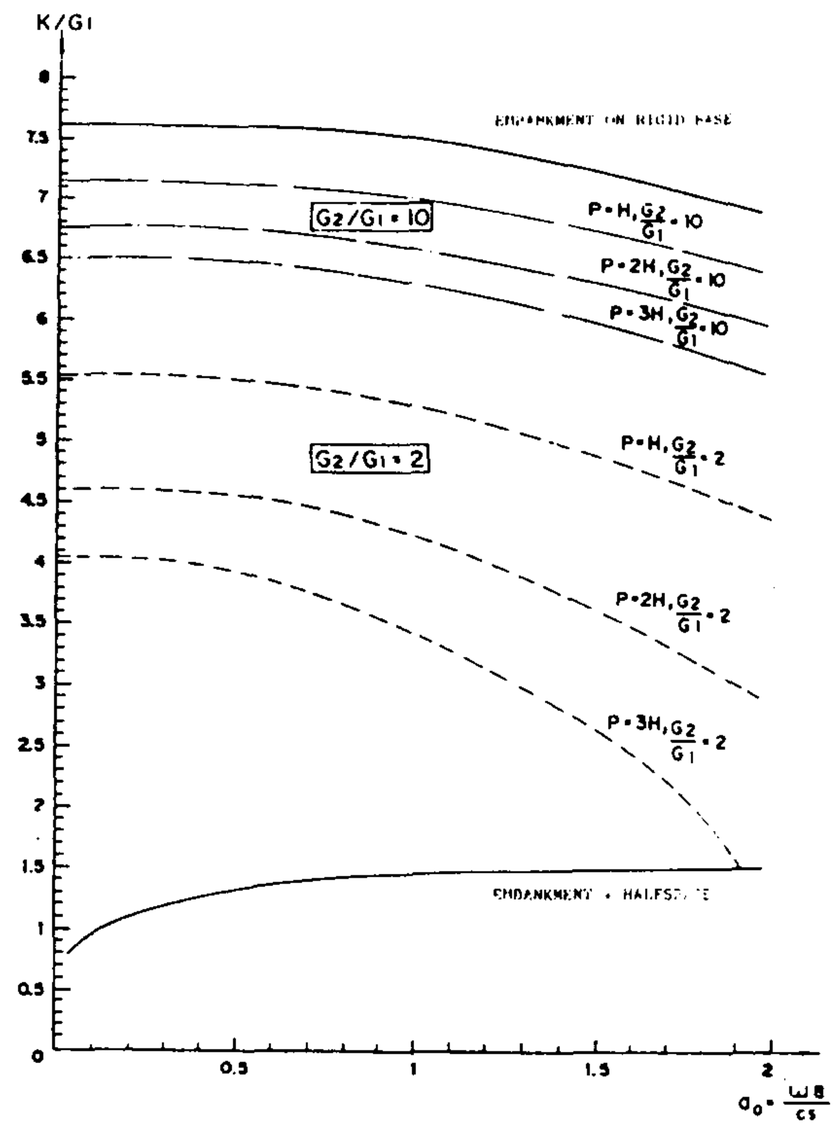

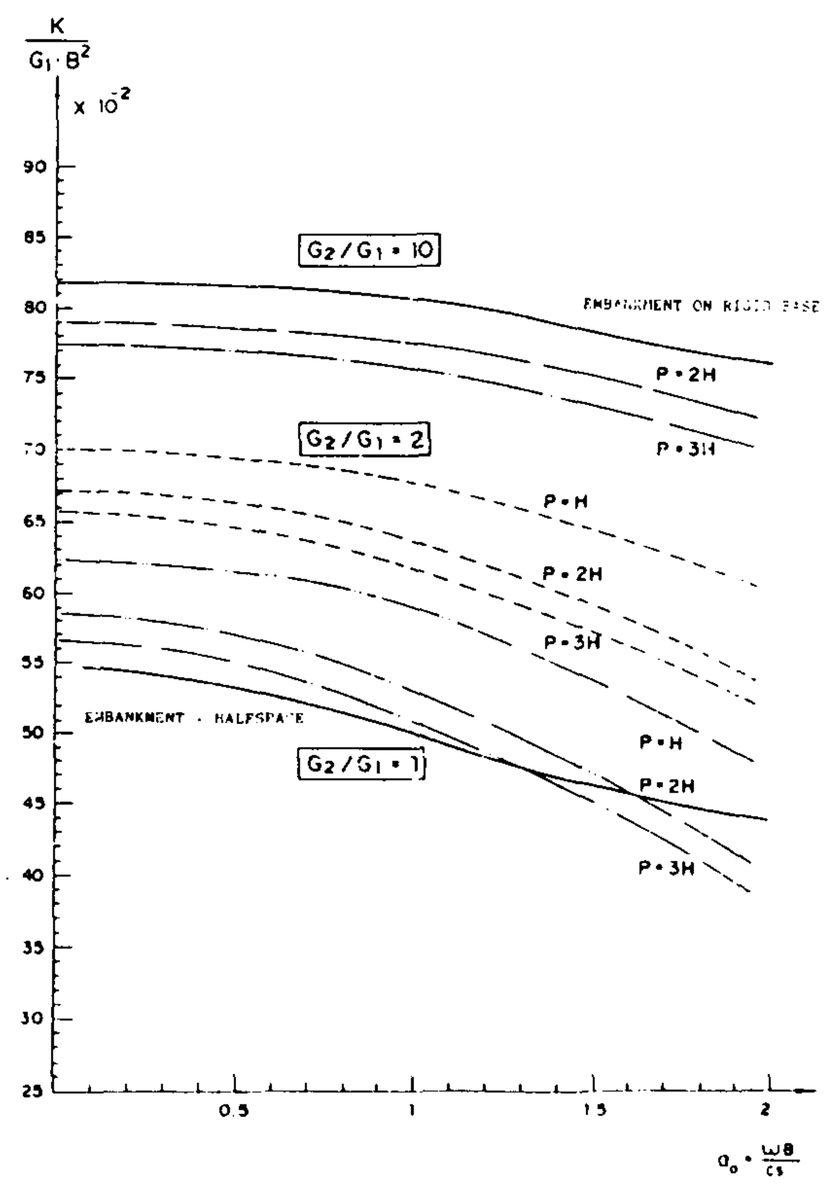

Figure 12. Vertical and rocking stiffness

For the case analyzed in reference 4 it was found that the natural adimensional frequency was about 2. For this value and a horizontal displacement the halfspace stiffness is 1/3 of that of the embankment on a rigid base what agrees with experimental findings.

On figures 13, 14 and 15 the imaginary parts divided by the adimensional frequency are plotted without factoring the internal damping effect.

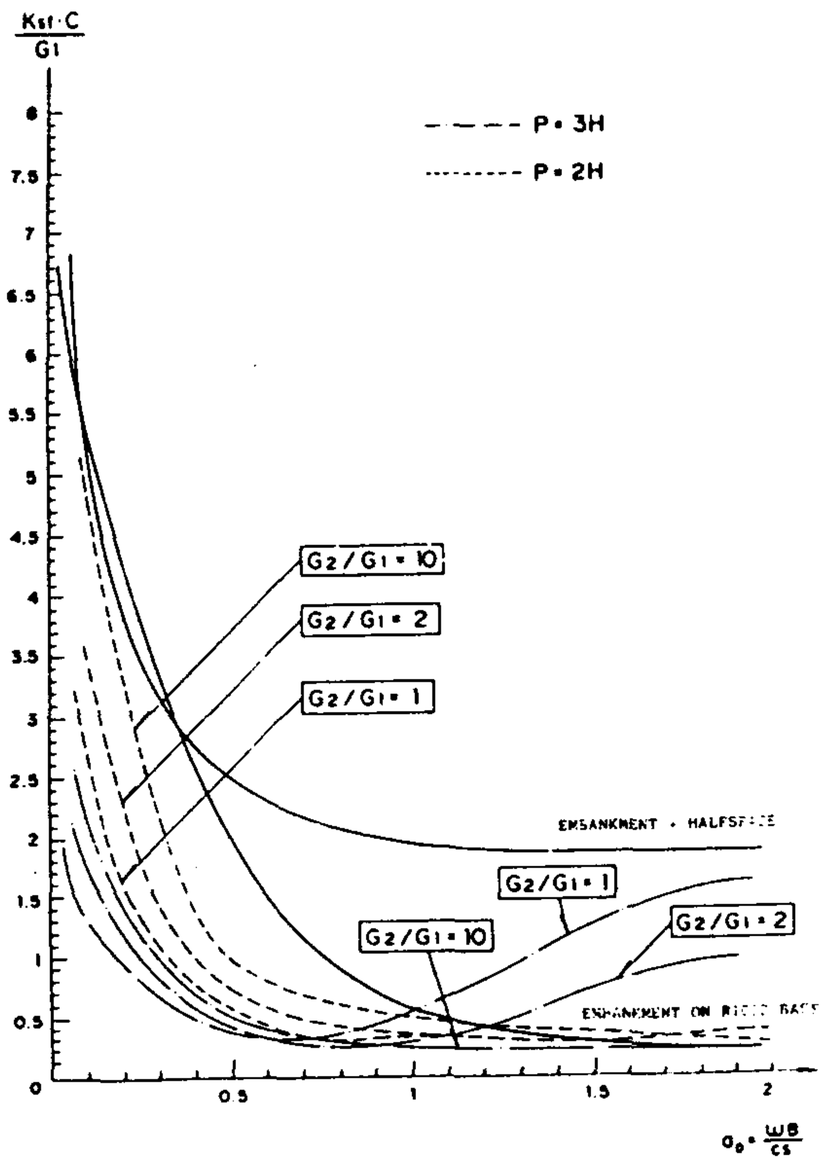

Figure 13. Vertical disipation

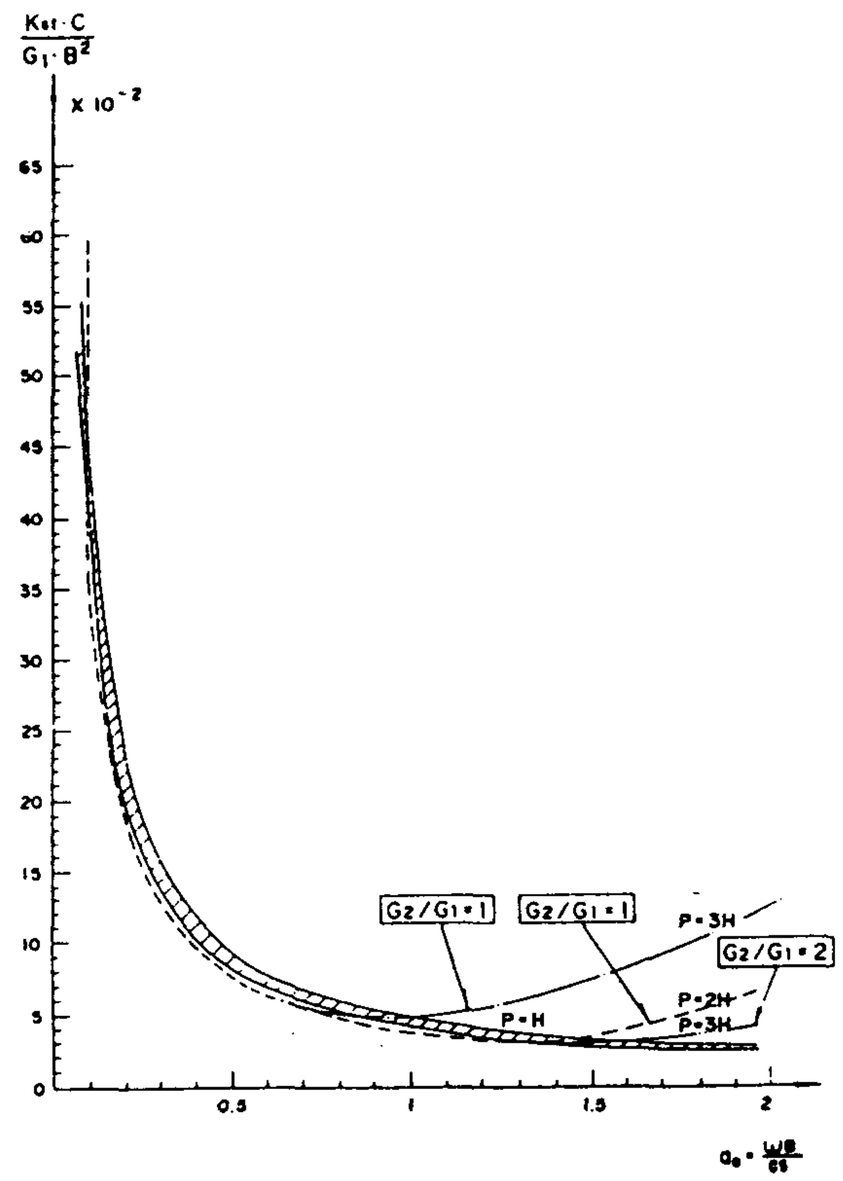

Figure 14. Rocking disipation

It is possible to see the difference between the halfspace and the trapezoid on rigid base cases which for the horizontal displacement amounts to a 6 fold value. In any case it is advisable to remember that 2_D damping is very large in comparison with that obtain for a 3_D situation.

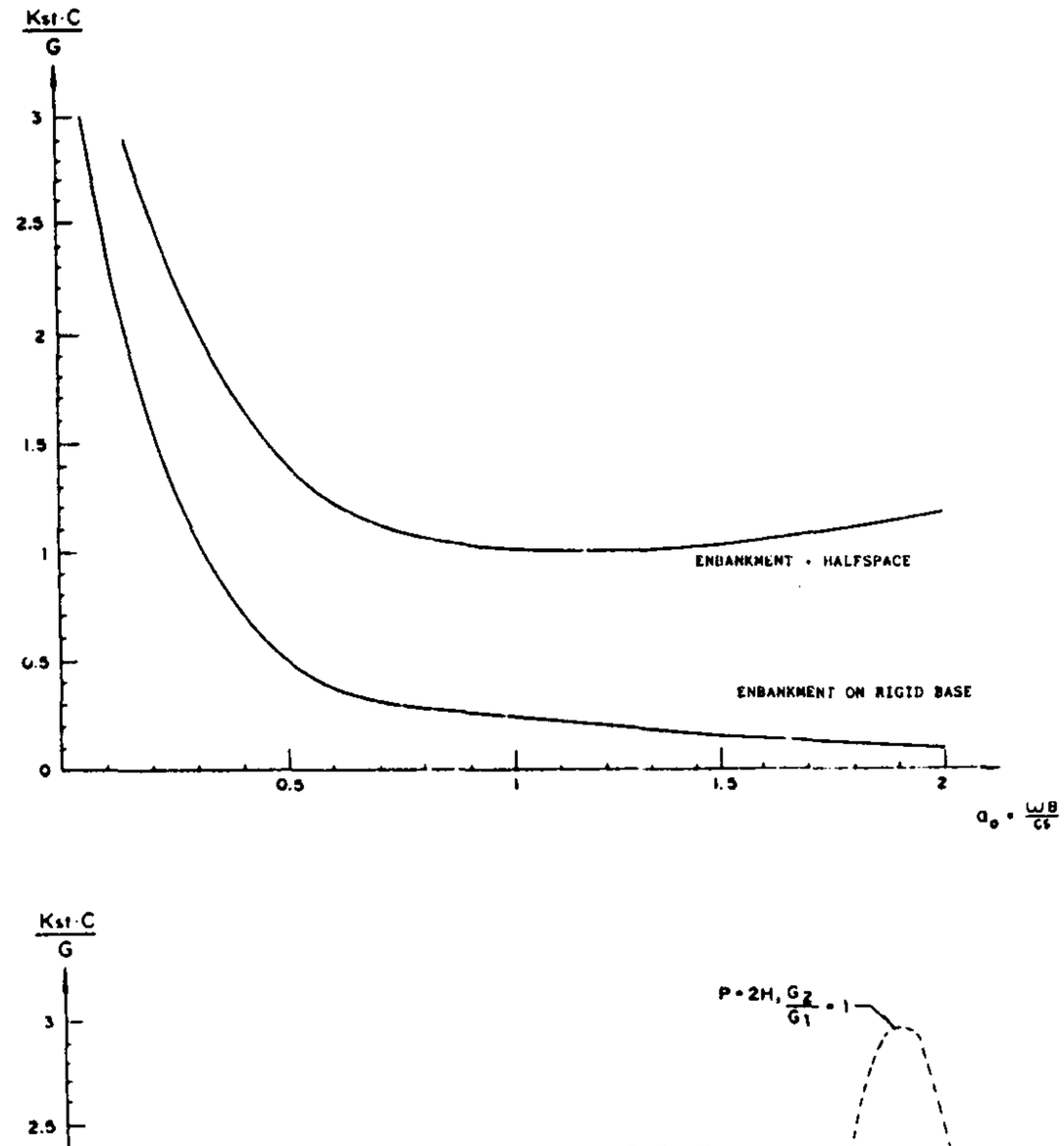

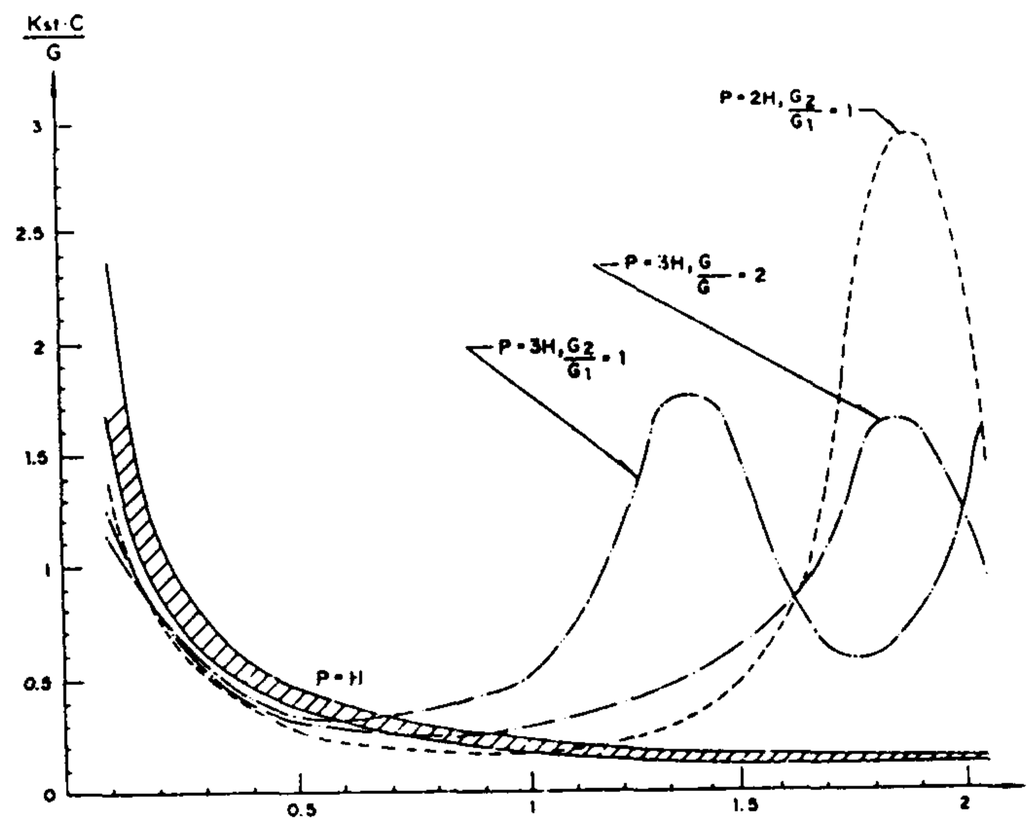

Figure 15. Horizontal disipation

Finally, figure 16 shows the meshes used for the analysis of a threedimensional exemple.

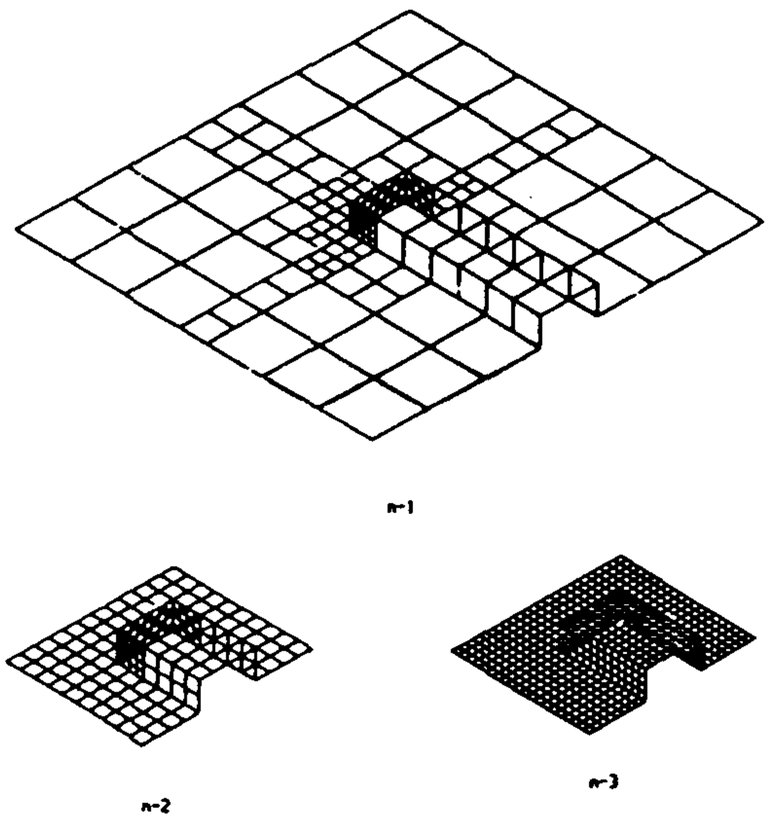

Figure 16

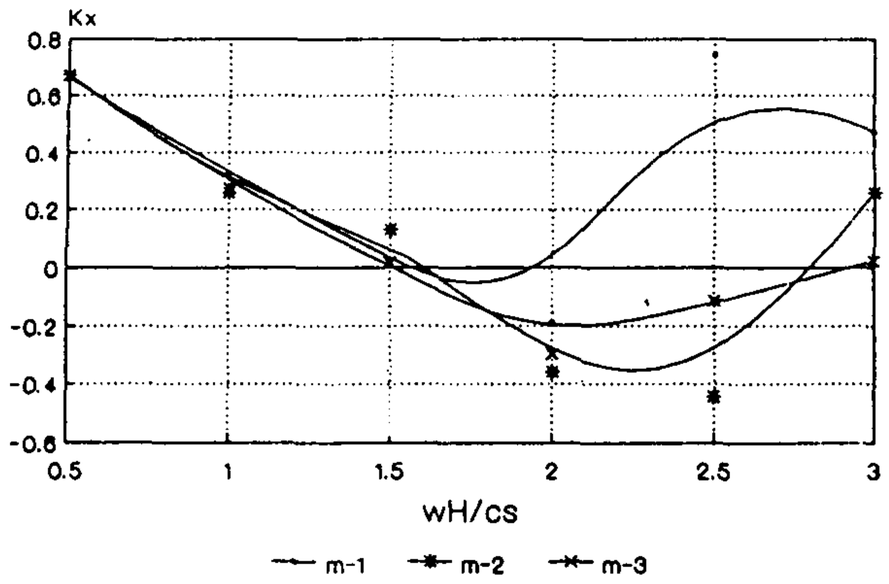

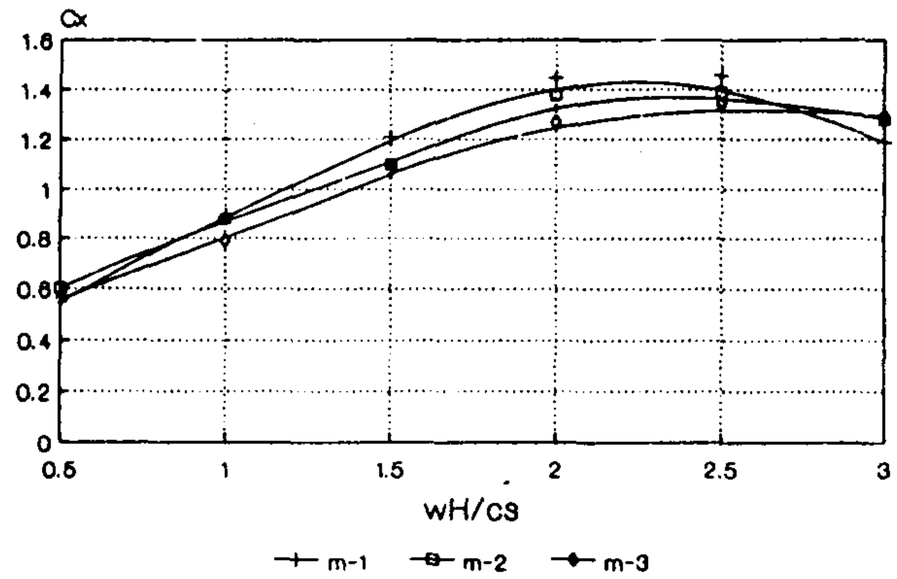

Figure 17

It is important to reduce as much as possible the computational effort so that several sizes and distributions have been tried. The comparative results can be seen in figure 17 where it can be observed that, at least a mesh of the type called 2 will have to be used to represent correctly the longitudinal behaviour.

For the transverse stiffness, figure 18 shows that even with the finer mesh it is possible to obtain very accurate results. It is also interesting to see that reduction,

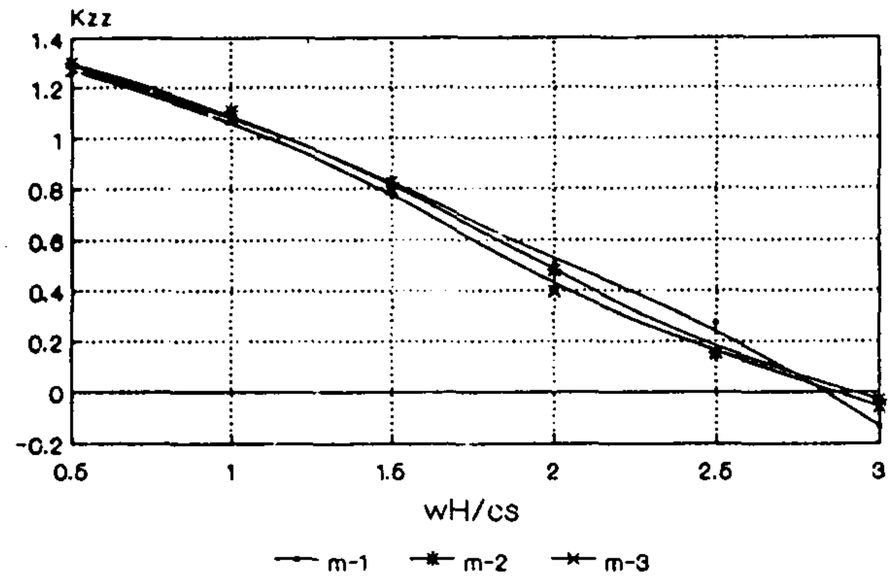

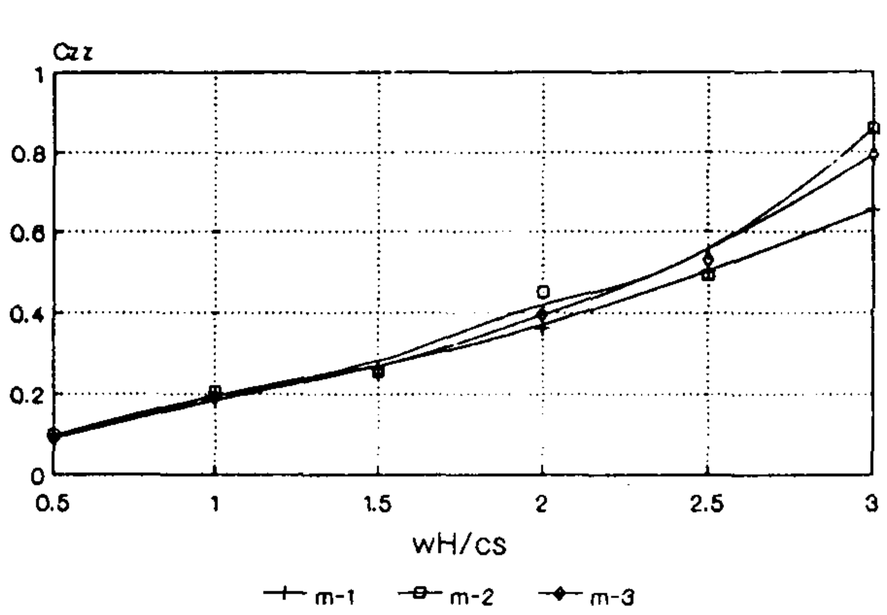

Figure 18

due to the dynamic in stiffness behaviour justifies the 1/3 finding of Wilson and also that the radiation damping presents values large enough to justify those obtained during the identification parameter study of Melolan Road Overpass without having to look for a nonlinear behaviour of the soil substructure.

4. CONCLUSSIONS

The aim of the paper is to show that it is possible to use realistic dynamic models to reproduce the sitffness and damping that has been detected in the abutment of real bridges that survived real earthquakes without apparent damage.

On the other hand the numerical technique used, the so-called Boundary Element Method, seems to be a proverful tool to analyze those kind of dynamic soil-interaction problems.

REFERENCES

1. AASHTO (1983):"Guide Specifications for seismic design of Highway bridges"
2. J.P. Wolf (1985): "Dynamic soil-structure interaction". Prentice Hall.
3. E.A. Maragakis et al (1989): "A simple nonlinear model for the investigation of the effects of the gap closure at the abutment joints of short bridges". Earth. Eng. Struct. Dynamics. Vool. 18; 1163-1178.

4a. J.C. Wilson & B.S. Tan (1990): "Bridge abutments: Formulation of simple model for earthquake response analysis" ASCE Jour ENg. Mech. Vol. 116 No. 8.

4b. Ditto: "Bridge abutments: Assesing their influence on earthquake response of Meloland Road Overpass" (Same reference).

5. J. Domínguez & E. Alarcón (1981): "Elastodynamics" Chap 7 in "Progress in Boundary Element Method". Ed. C. Brebbia. Pub. Pentech Press.
6. E. Alarcón; J.J. Cano; J. Domínguez (1989): "Boundary Elements approach to the dynamic stiffness of circular foundations". Inst. Jour. Num. Analyt. Meth. Geomech. Vol 13; 645-664.
7. A. Martínez; E. Alarcón; Mª.S. Gómez-Lera; F. Chirino (1992): "Application of the Boundary Element Method to the analysis of Bridge Abutments".
8. H.Tajimi (1973):"Dynamic earth pressure on basement wall". World Conference on Earthquake Engineering. Roma.
9. J.H. Wood (1973): "Earthquake-induced soil pressures on structures". Ph. D. Thesis. Caltech. Pasadena.